High position resolution gamma-ray imagers consisting of a monolithic MPPC array with submillimeter pixelized scintillator crystals

Takuya Kato, Jun Kataoka, Takeshi Nakamori, Aya Kishimoto, Seiichi Yamamoto, Kenichi Sato, Yoshitake Ishikawa, Kazuhisa Yamamura, Sigeyuki Nakamura, Nobuyuki Kawabata, Hirokazu Ikeda, Kei Kamada

***Abstract*—We report on the development of two versatile, high spatial resolution gamma-ray imagers for medical imaging. One is a compact gamma-ray camera, the other is a tweezers type coincidence imaging system. These applications consisting of a large-area monolithic Multi-Pixel Photon Counter (MPPC) and submillimeter pixelized scintillator matrices. The MPPC array has 4×4 channels with a three-side buttable, very compact package. Each channel has a photosensitive area of 3×3 mm^2 and 3600 Geiger mode avalanche photodiodes (APD). For a typical operational gain of 7.5×10^5 at +20 degrees, gain fluctuation over the entire MPPC device is only $\pm 5.6\%$, and dark count rates (as measured at the 1 p.e. level) amount to $\leq$400 kcps per channel. We particularly selected Ce-doped $(Lu,Y)_2(SiO_4)O$ (Ce:LYSO) and a brand-new scintillator, Ce-doped $Gd_3Al_2Ga_3O_{12}$ (Ce:GAGG) due to their high light yield and density. To improve the spatial resolution, these scintillators were fabricated to 22×22 or 15×15 matrices of 0.5×0.5 mm^2 pixels. These scintillator matrices were coupled to the MPPC array with an acrylic light guide with 1 mm thick, and signals were read out using the charge division resistor network, which compiles signals into four position-encoded analog outputs. The spatial resolution of 1.2 mm was achieved with the compact gamma-ray camera using collimated ^{57}Co source, and a radiography image of a bearing was successfully obtained. On the other hand, the spatial resolution of 1.1 mm was achieved with the coincidence imaging system using a ^{22}Na source. Furthermore the experimental measurements for a PET scanner was performed, and the spatial resolution of 0.91 mm was achieved. These results suggest that the gamma-ray imagers has excellent potential for their uses as a high spatial medical imaging, and also be promising for positron emission tomography (PET).**

Manuscript received ?????

T. Kato, J. Kataoka, T. Nakamori, A. Kishimoto are with the Research Institute for Science and Engineering, Waseda University, Shinjuku, Tokyo 169-8555, Japan (e-mail: katou.frme.8180@asagi.waseda.jp; kataoka.jun@waseda.jp; nakamori@anoi.waseda.jp; daphne3h-aya@ruri.waseda.jp).

S. Yamamoto is with Nagoya University Graduate School of Medicine, 1-1-20, Daikominami, Higashi-ku, Nagoya-shi, Aichi 461-8673, Japan (e-mail: s-yama@met.nagoya-u.ac.jp).

K. Sato, Y. Ishikawa, K. Yamamura, S. Nakamura, N. Kawabata are with Hamamatsu Photonics, K.K., 1126-1, Ichino-cho, Higashi-ku, Hamamatsu-shi, Shizuoka 435-8558, Japan (e-mail: k-sato@ssd.hpk.co.jp; yoshi-i@ssd.hpk.co.jp; yamamura@ssd.hpk.co.jp; sigeyuki@ssd.hpk.co.jp; kawa-bata@hq.hpk.co.jp).

H. Ikeda is with ISAS/JAXA, 3-1-1, Yoshinodai, Chuo-ku, Sagamihara-shi, Kanagawa, 252-5210, Japan (e-mail; ikeda.hirokazu@jaxa.jp).

K. Kamada is with Materials Research Laboratory, Furukawa Co., Ltd., 1-25-13, Kannondai, Tsukuba, Ibaraki 305-0856, Japan (e-mail; k-kamada@furukawakk.co.jp).

I. Introduction

Positron emission tomography (PET) imaging is a well-established method of detecting cancers and diagnosing Alzheimer's in its early stages [1]. Currently, many advantageous aspects of PET combined with Magnetic Resonance Imaging (MRI) have being proposed (MRI-PET), and with prototypes now being tested as MRI produces an excellent soft-tissue contrast and anatomical detail without additional radiation [2]–[4]. However, a Photo-Multiplier Tube (PMT) incorporated in conventional PET scanners is difficult to use within the high magnetic field of MRI. Moreover, the large-size PMT-based PET not only complicates use in narrow MRI tunnels but also limits the spatial resolution far from the theoretical limits of PET resolution.

A Multi-Pixel Photon Counter (MPPC), also known as a Silicon Photo-Multiplier (SiPM), is a promising semiconductor photodetector for PET. It is insensitive to magnetic fields and compact. In addition, it has a gain comparable to that of PMTs at up to the $10^5 \sim 10^6$ level, resulting in good signal-to-noise (S/N) ratio and excellent timing property [5]. These great advantages make the MPPC an ideal photosensor for MRI-PET as well as for Time Of Flight (TOF) applications [6], [7].

A high-resolution MRI-PET/TOF-PET technique utilizing the MPPC array is now being developed. We previously developed and tested a monolithic, three-side buttable 4×4 MPPC array with submillimeter pixelized Ce-doped $(Lu,Y)_2(SiO_4)O$ (Ce:LYSO) and Ce-doped $Gd_3Al_2Ga_3O_{12}$ (Ce:GAGG) scintillator matrices [8]. In the position histograms, each scintillator pixel is clearly resolved, suggesting the possibility of its use for submillimeter high resolution gamma-ray imaging application. In this paper, we developed two MPPC-based gamma-ray imagers; one is a compact gamma-ray camera [9], the other is a tweezers type coincidence imaging system [10]. Furthermore, we evaluated a spatial resolution of prototype gantry for a PET scanner.

II. Materials and methods

A. 4×4 MPPC array

Fig. 1 shows a picture of the monolithic 4×4 MPPC array [11] developed in this paper. The MPPC array was designed and developed for future applications in nuclear medicine (such as PET scanners) by Hamamatsu Photonics K.K.. Each channel has a photosensitive area of 3×3 mm^2 and 60×60

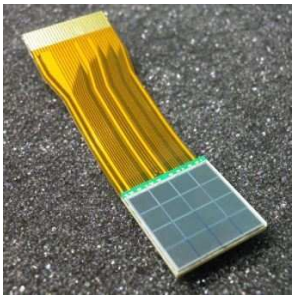

Fig. 1. Photo of the 4×4 MPPC array developed in this paper.

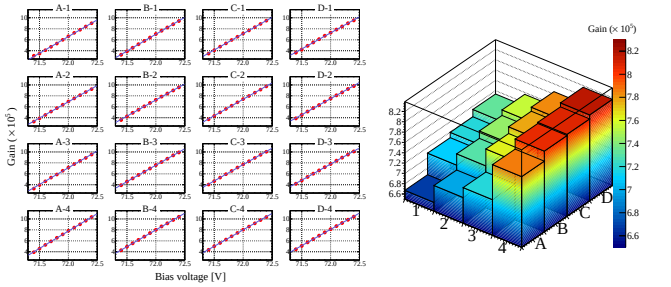

Fig. 2. $left$: Gain variation as a function of bias voltage for all pixels from 71.4 to 72.4 V, measured at +20 degrees. $right$: Gain distribution at the operation voltage of 72.01 V

Geiger mode avalanche photodiodes (APDs) arranged with a pitch of 50 μm. The gap between each channel is only 0.2 mm thanks to the monolithic structure. The MPPC array is placed on a surface-mounted package measuring 14.3 by 13.6 mm, and fabricated into a three-side buttable structure, that is, the distance from the photosensitive area to the edge of the package is only 500 μm. An excellent gain uniformity ($\pm 5.6\%$) (Fig. 2) and very low dark count rates ($\leq$400 kcp, due to the 1 p.e. level) have been achieved at an averaged gain of 7.5×10^5, measured at +20 degrees. Table I lists the other basic characteristics of the MPPC array.

Also, the energy and time resolutions were obtained as $11.5 \pm 0.5\%$ (FWHM at 662 keV photoelectric peak) and 493 ± 22 ps (FWHM), respectively when the MPPC array were optically coupled with a Ce:LYSO scintillator [8].

B. Scintillators

To fabricate gamma-ray imaging applications, we selected Ce:LYSO and Ce:GAGG scintillators. Ce:LYSO, which is one of the most popular scintillator at present in medical imaging, has features such as high light yield (75% of Tl:NaI), short scintillation decay time (40 nsec) and high density (7.4 g/cm^3) greater than $Bi_{12}Ge_3O_{20}$ (BGO) (7.1 g/cm^3) [12]. However, Ce:LYSO contains a considerable amount of self radiation emitted from ^{176}Lu. Alternatively, a brand-new scintillator, Ce:GAGG also have very high light yield and short scintillator decay time, and it is noteworthy that Ce:GAGG is absence of self radiation [13]. Table II lists the other basic characteristics of the Ce:LYSO and the Ce:GAGG scintillators.

Fig 3 ($right$) shows ^{137}Cs spectra obtained by using a $3 \times 3 \times 10$ mm^3 Ce:LYSO and Ce:GAGG (Fig 3 ($left$)) crystals with a 50 μm-type 3×3 mm^2 MPPC

TABLE I
SPECIFICATION OF THE 4×4 MPPC ARRAY AT $+25$ DEG

Parameters	Specification
Number of elements [ch]	4×4
Effective active area / channel [mm]	3×3
Pixel size of a Geiger-mode APD [μm]	50
Number of pixels / channel	3600
Typical photon detection efficiency[1](λ=440 nm) [%]	50
Typical dark count rates / channel [kcps]	≤ 400
Terminal capacitance / channel [pF]	320
Gain (at operation voltage)	7.5×10^5

[1] including cross-talk and after-pulse contributions

TABLE II
BASIC CHARACTERISTICS OF THE CE:LYSO AND CE:GGAG SCINTILLATORS

	Ce:LYSO	Ce:GGAG
Density [g/cm^3]	7.10	6.63
Light yield [photons/MeV]	25,000	46,000
Decay time [nsec]	40	88(91%) and 258(9%)
Peak wavelength [nm]	420	520

(Hamamatsu:S10362-33-050C), measured at +20 degrees. The MPPC was operated at the gain of 7.5×10^5. Typically, MPPCs are most sensitive within the range of 350-500 nm [14]. In this sense, a emission of the Ce:GAGG, peaking at 520 nm is not favorable, but the output charges from the MPPC with the Ce:GAGG was about 21% larger than that of the Ce:LYSO due to the high light yield of Ce:GAGG. The Energy resolution for the 662 keV photoelectric peak were 9.9% and 7.9% for the Ce:LYSO and the Ce:GAGG after linearity correction [15], respectively. Their high light yield should realize the better energy resolution, and moreover, good spatial resolution when they are fabricated to small pixels and read out by a charge division resistor network [9].

C. Configuration of compact gamma camera

The compact gamma camera consists of the MPPC array with a Ce:GAGG scintillator matrix, namely, 22×22 matrix of 0.5×0.5 mm^2 pixels (Fig. 4 ($left$)). Each pixel is divided with a reflective $BaSO_4$ layer 0.1 mm thick, and the total size of the scintillator matrix is $13.1 \times 13.1 \times 10$ mm^3. The scintillator matrix were optically coupled to the MPPC array with an acrylic light guide 1 mm thick, which distributes scintillator photons across multiple MPPC array channels.

The signals from the MPPC array was compiled into four position-encoded analog outputs by using a charge division resistor network [8]. The four signals were fed into Quad Linear FAN IN/OUT (Phillips MODEL 6954) and divided into two lines. One was directly fed into the charge sensitive ADC (HOSHIN V005; hereafter CSADC), with the other being summed over four signals to generate a trigger with the non-update discriminator (Technoland N-TM 405).

The tungsten sheet, which is the complex material of the powder of W and the resins and has a stopping power equal to a Pb, with a 1 mm diameter and 3 mm long hole was used as a gamma-ray collimator. The collimator was placed at the distance of 12 mm from the surface of the Ce:GAGG matrix (Fig 4 ($right$)). The Ce:GAGG matrix was not enclosed any shields. The spatial resolution of this gamma camera was evaluated by means of taking images of the collimated

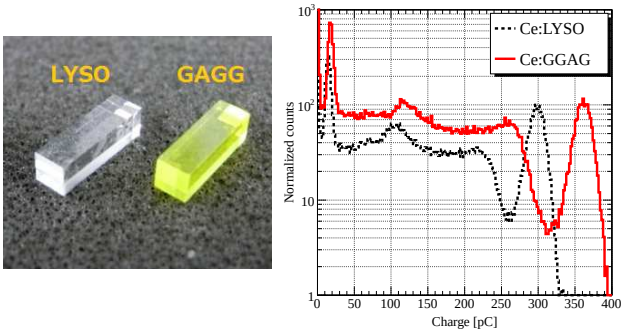

Fig. 3. $left$: Photo of the $3 \times 3 \times 10$ mm^3 Ce:LYSO and the Ce:GAGG scintillators. $right$: Energy spectra of ^{137}Cs source. Red line and dashed black line represent the Ce:GAGG and Ce:LYSO, respectively.

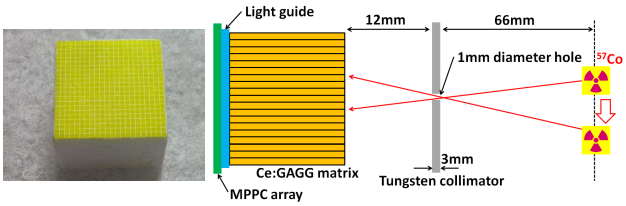

Fig. 4. $left$: Photo of the 22×22 of 0.5×0.5 mm^2 Ce:GAGG matrix. $right$: Configuration of the compact gamma camera.

122 keV gamma-ray irradiated by a ^{57}Co source. The ^{57}Co was placed at the distance of 66 mm from the surface of tungsten collimator, and its position was flexibly controlled parallel to the tungsten collimator using the X-stage (SGSP 20-85, Sigma Koki) to evaluate the resolution performance, while the accuracy of the stage controllers was 1 μm/pulse. The images were taken by changing the position of ^{57}Co source at 3.46 mm intervals (corresponding to a viewing angle of 3 degrees). The image quality without the collimator was also evaluated by taking a radiography image of a small (10 mm diameter) ball bearing made of stainless steel, irradiated by the ^{57}Co source.

D. Configuration of tweezers type imaging system

The tweezers type imaging system has two phosphor sandwich (phoswich) gamma-ray detector blocks consisting of the MPPC arrays, Ce:LYSO and Ce:GAGG scintillator matrices. These scintillator matrices are composed of 15×15 matrices of 0.5×0.5 mm^2 pixels optically separated by $BaSO_4$ layer 0.1 mm thick (Fig 5 ($left$)). The total size of the scintillator matrices are $9.7 \times 9.7 \times 5$ mm^3, and the configurations of each matrix is completely matched. The Ce:LYSO matrix was coupled to the MPPC array with the acrylic light guide 1 mm thick, and the Ce:GAGG matrix was coupled to the other side of the Ce:LYSO matrix (Fig 5 ($right$)). The detector block is capable of two-layer Depth of Interaction (DoI) measurement by identifying in which scintillator matrices the event occured. Two detector blocks were then attached on acrylic tongs, and form a tweezers type coincidence gamma-ray imager (Fig 6).

Output signals from the MPPC arrays were fed into a coincidence DAQ system developed by ESPEC TECHNO CORP. after compiled four position-encoded analog outputs

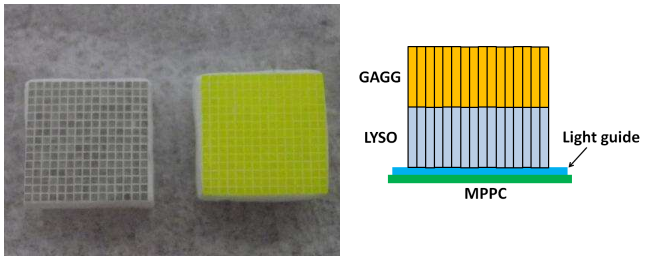

Fig. 5. $left$: Photos of the 15×15 of 0.5×0.5 mm^2 Ce:LYSO (left side) and Ce:GAGG (right side) matrices. $right$: Configuration of the two-layer phoswich gamma-ray detector block. The MPPC array, the acrylic light guide, the Ce:LYSO and the Ce:GAGG scintillator matrices are optically coupled each other.

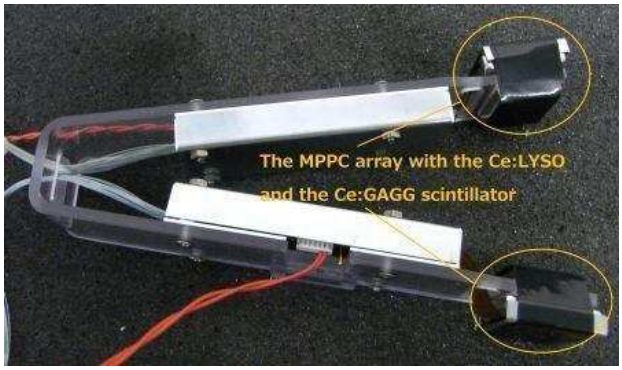

Fig. 6. Photo of the developed tweezers type coincidence imager using a pair of MPPC arrays coupled with the 0.5×0.5 mm^2 Ce:LYSO and Ce:GAGG scintillator matrices.

(x direction; X_+ and X_-, y direction; Y_+ and Y_-) by the summing operational amplifiers [9], [16]. The compiled signals were digitized by a 100 M samples/s ADC (AD9218 BST-105), and then, processed by field-programmable gate arrays (FPGAs). When the digital signals were over the threshold of digital comparator, the signals are integrated with two different integration time (130 ns and 320 ns). The positional distributions were calculated by the anger-logic; $x = (X_+/(X_+ + X_-))$ and $y = (Y_+/(Y_+ + Y_-))$, and the energy was delivered from the sum of four signals. If the timing signals from the MPPC arrays coincidence within the time-window of 20 ns and their energies are within the energy-window of 511 ± 102.2 keV, the HIT address, timing and valid flag are stored in a memory for use in creating list-mode data.

In a performance test, a ^{22}Na source (0.593 MBq at the measurement date) was set between the two detector blocks. The ^{22}Na source was doped within the central 0.25 mm ϕ region and could hence be regarded as a point source.

E. Configuration of prototype gantry for a PET scanner

We plan to fabricate a PET scanner using the MPPC arrays and the fine scintillator matrices. In a preliminary performance test, two MPPC-based PET detectors consisting of the MPPC arrays, 0.5×0.5 mm^2 Ce:LYSO and Ce:GAGG scintillator matrices described in section II-D were used. The photo of the experimental setup is provided in Fig 7. The 0.25 mm ϕ ^{22}Na point source was located between the MPPC-based PET detectors, and its position was then flexibly controlled

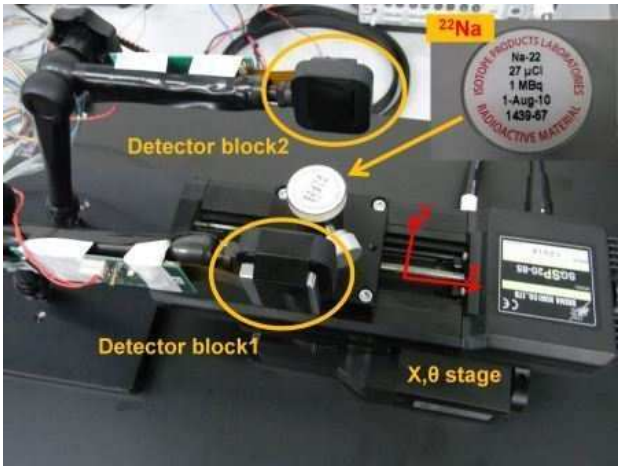

Fig. 7. Experimental setup of the prototype system for a PET scanner. The distance between two detector blocks is 70 mm.

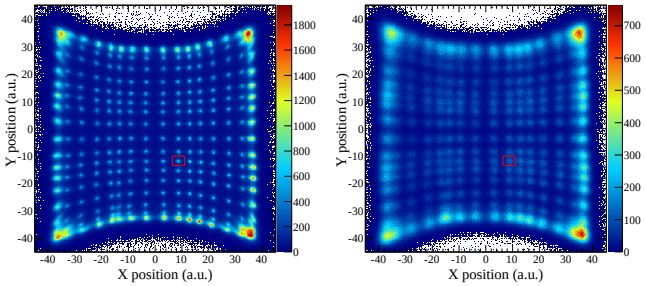

Fig. 8. Flood images of 22×22 of 0.5×0.5 mm^2 Ce:GAGG scintillator matrix with a ^{137}Cs ($left$) and a ^{57}Co ($right$) source.

by the X-stage and the θ-stage (SGSP 80Y-AW, Sigma Koki), whose accuracy was 2.5×10^{-3} deg/pulse. Coincidence events were taken at ten positions by changing the roll angle (θ) at 18 degree intervals from 0 to 162 degrees. At each step, data were taken for 10 minutes.

III. Results

A. Compact gamma-ray camera

1) flood image: Fig 8 shows flood images obtained for the 22×22 Ce:GAGG scintillator matrix by irradiation a ^{137}Cs and a ^{57}Co source. The flood images show overlapping peaks of the side pixels, as the total size of scintillator matrix is a bit larger than the sensitive area of the MPPC array. And scintillation photons from the side pixels were only delivered into the side channels of the MPPC array. However, the central pixels were successfully resolved in the flood images. In the flood image of the ^{137}Cs source, the peaks are narrower than that of the ^{57}Co source. This is because the 662 keV gamma-ray irradiated by ^{137}Cs source generate greater amount of charges from the MPPC array. The greater the charges involved, naturally, the better positional statistical error.

We extracted energy spectra from only resolved pixels by selecting events around the corresponding peaks in the flood images. Fig 9 shows example spectra of the ^{137}Cs and the ^{57}Co source after the linearity correction. The energy resolution for 662 keV and 122 keV were 14.2% and 21.8%, respectively.

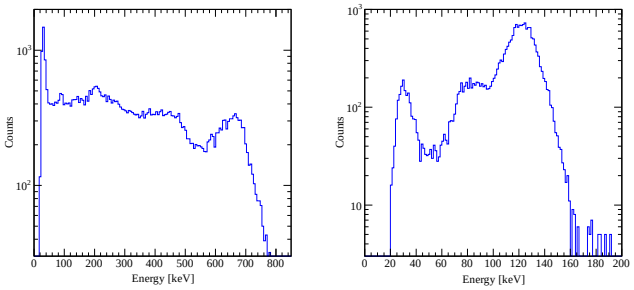

Fig. 9. Example energy spectra of a ^{137}Cs and a ^{57}Co source for 0.5×0.5 mm^2 Ce:GAGG matrix extracted from the red square in Fig 8.

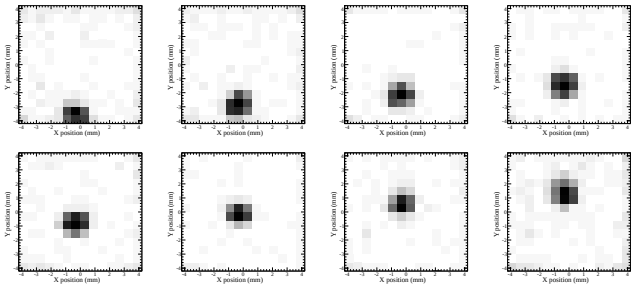

Fig. 10. Images of collimated ^{57}Co source. From upper left to lower right, the 3.46 mm movement of the ^{57}Co source are presented.

A energy window of 122 keV $\pm$ FWHM/2 (corresponding to $\sim$13 keV) was applied when the collimated ^{57}Co and the radiography images were taken.

2) pinhole image: The images of the collimated ^{57}Co source was shown in Fig 10. The 3.46 mm movement of the ^{57}Co source was clearly distinguished. The spatial resolution at the center of field of view was 1.2 mm (FWHM) (without correction of the collimator hole diameter of 1 mm).

3) radiography image: Fig 11 ($right$) shows the radiography image of the ball bearing, which was smoothed by the gaussian filter of σ = 0.15 mm. The structure of the ball bearing including 1 mm ball can be clearly resolved.

B. Tweezers type coincidence imager

1) flood image: Fig 12 show flood image results obtained for 15×15 Ce:LYSO and Ce:GAGG scintillator matrices individually coupled to the MPPC array. Fig 13 show example energy spectra extracted from the flood images. The energy resolutions for 662 keV, which were not corrected for non-linearity, were 14.0% and 9.4% for Ce:LYSO and Ce:GAGG, respectively.

2) signal selection: Fig 14 shows the wave form corresponding to 511 keV photoelectric absorption by the Ce:LYSO and Ce:GAGG. The decay time of the signals, which includes the scintillator decay time and the MPPC response, are approximately 70 ns and 150 ns for the Ce:LYSO and the Ce:GAGG, respectively. Fig 15 ($left$) shows the 2D energy plot; x-axis and y-axis correspond to the 130 ns and 320 ns ADC channel, respectively. For the 130 ns integration time, the signals of the Ce:LYSO is same or a little bit larger than that of Ce:GAGG as shown in Fig 14, while, for the 320 ns

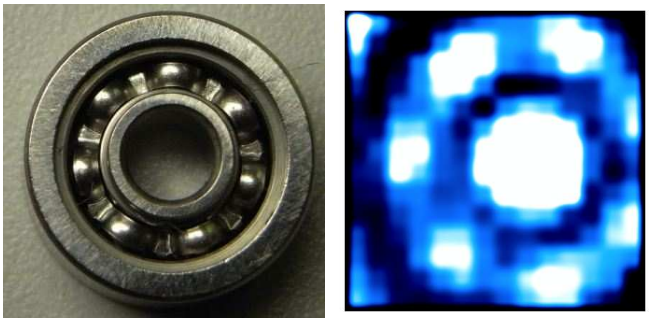

Fig. 11. $left$: Photo of the 10 mm diameter ball bearing. $right$: Radiography image of the ball bearing smoothed by the gaussian filter of σ = 0.15 mm.

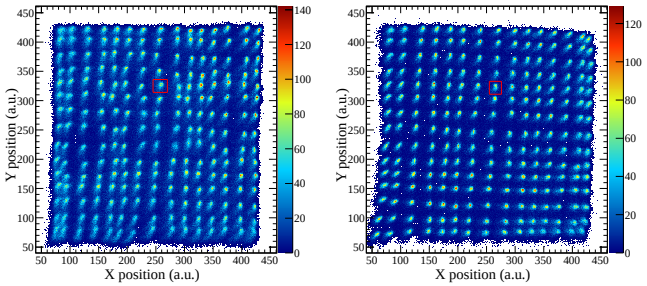

Fig. 12. Flood images of 15×15 of 0.5×0.5 mm^2 Ce:LYSO ($left$) and Ce:GAGG ($right$) scintillator matrices with a ^{137}Cs source.

integration time, the signals of the Ce:GAGG is larger. As a result, the events of each scintillator trace two different lines in 2D energy plot. Fig 15 ($right$) show the 130 ns to 320 ns ADC channel ratio. If the Fast(130 ns)/Slow(320 ns) ratio is over 0.84, the event is regarded as being originated from the Ce:LYSO, and conversely if the Fast/Slow ratio is under 0.84, the event is regarded as the Ce:GAGG event. Fig 16 show the energy spectra after event selection, and each scintillator event can be effectively distinguished.

3) Image reconstruction: Fig 17 show the sinogram transformed from the list mode data. The two interaction positions in each coincidence event, which define the Lines of Response (LoR), were randomly determined according to the uniform distribution within the hit pixels. The simple planar image reconstruction [17] were performed with the intersection of the all LoRs and the plane centrally located between the two detectors. Fig 18 shows the planar image of the ^{22}Na point source. The non-DoI image were reconstructed by reckoning the Ce:LYSO and the Ce:GAGG pixels as a single pixel. When the DoI information was applied, the spatial resolution were 1.1 mm (x direction) and 1.4 mm (y direction), which was slightly better than the case of non-DoI (1.2mm (x direction) and 1.5 mm (y direction)).

C. Prototype gantry for a PET scanner

Maximum Likelihood-Expectation Maximization (MLEM) [18] method was used to reconstruct images. Fig 19 shows sinograms and the resultant reconstructed images obtained for the center and off-center (3.0 mm), respectively. The radial spatial resolution was estimated at 0.91 and 0.94 mm for the center and 3.0 mm off-center, respectively.

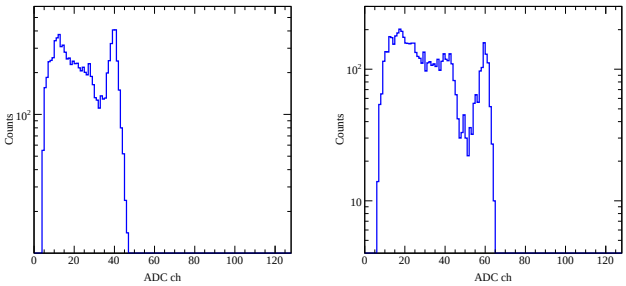

Fig. 13. Example energy spectra for Ce:LYSO ($left$) and Ce:GAGG ($right$) matrices, extracted from the red square in Fig 12.

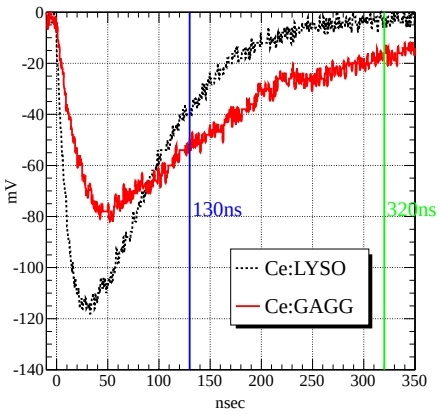

Fig. 14. Wave forms of the Ce:LYSO and the Ce:GAGG scintillator, corresponding to 511 keV photoelectric absorption event. Red line and dashed black line represent the Ce:GAGG and Ce:LYSO, respectively.

IV. Conclusion

In this work, we developed two versatile high spatial resolution gamma-ray cameras, which both achieved $\sim$1 mm spatial resolutions. These gamma-ray cameras consist of the 4×4 MPPC arrays and submillimeter pixelized scintillator matrices. The MPPC arrays have fine gain uniformity of $\pm 5.6\%$ and very low dark count rates of ≤ 400 kcps as measured at +20 degrees. Moreover, its compactness due to the monolithic and three-side buttable structure is suit for the compact medical imaging devices. For the compact gamma camera, 0.5×0.5 mm^2 Ce:GAGG scintillator matrix was used. The spatial resolution of 1.2 mm was achieved for the collimated ^{57}Co image at the center of the field of view. For the tweezers type coincidence imager, 0.5×0.5 mm^2 Ce:LYSO and Ce:GAGG scintillator matrices were used for phoswich detector. In the 2D energy plot, optical signals from the Ce:LYSO and the Ce:GAGG can be effectively distinguished. The spatial resolution of 1.1 mm was achieved for the simple planar image reconstruction when the DoI information was applied. In the preliminary measurement for a PET scanner, we used two detectors consisting of the MPPC arrays, the Ce:LYSO and the Ce:GAGG scintillator matrices with changing the roll angle. The radial spatial resolutions of 0.91 mm (center) and 0.94 mm (3 mm off-center) were achieved from a MLEM reconstructed images. These results suggest that a

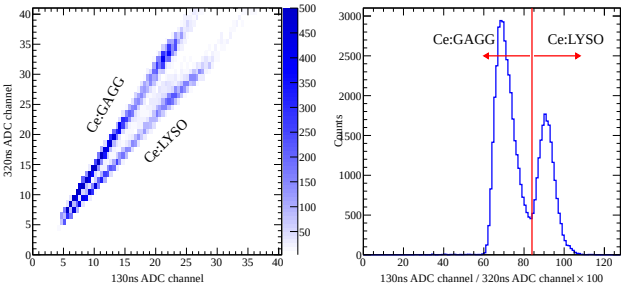

Fig. 15. $left$: 2D energy plot. x and y axis represent the 130 ns and 320 ns ADC channel, respectively. $right$: 130 ns to 320 ns ADC channel ratio. Right peak and left peak represent the Ce:GAGG and Ce:LYSO events, respectively.

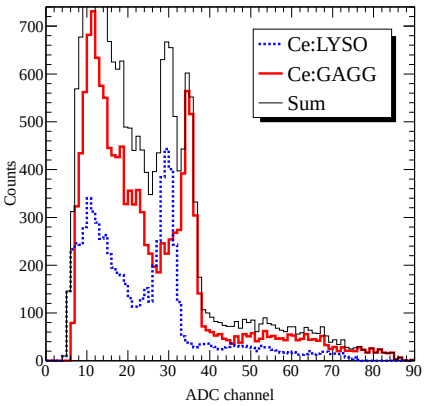

Fig. 16. Energy spectra distinguished from 2D energy plot. Black line, bold red line and dashed bold blue line represent the sum, Ce:GAGG and Ce:LYSO spectra, respectively.

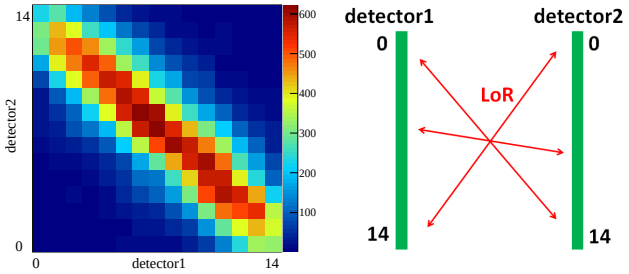

Fig. 17. $left$: Coincidence diagram constructed between two detector blocks. $right$ Schematic chart for the experimental setup, seen from the top view.

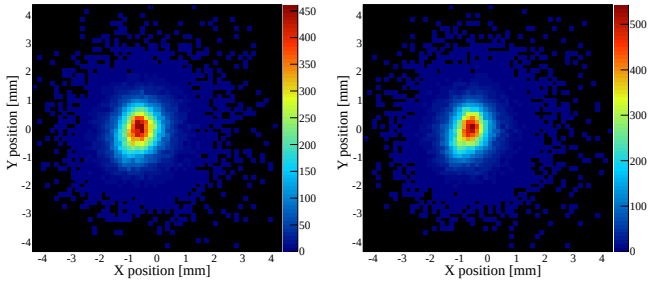

Fig. 18. The reconstructed planar images applied non-DoI ($left$) and DoI ($right$) information.

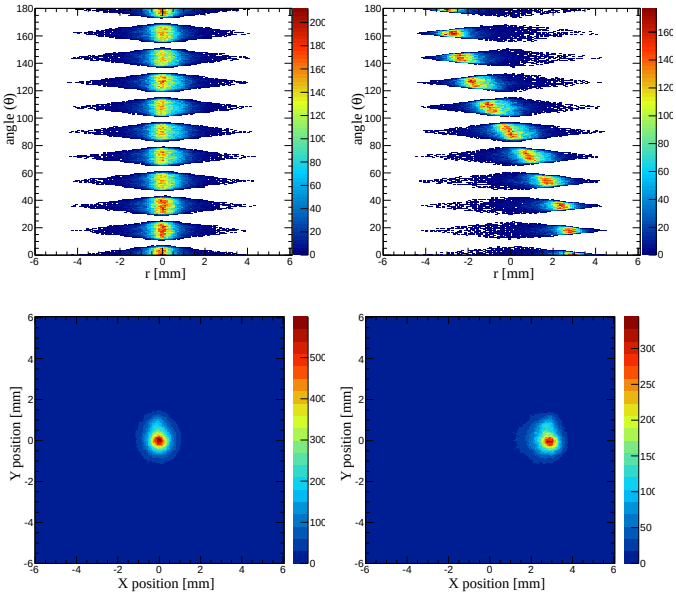

Fig. 19. Sinograms and reconstructed images by MLEM algorithm, measured with a ^{22}Na point source placed at center ($left$) and off-axis position x = 3 mm ($right$).

monolithic MPPC array coupled with submillimeter pixelized Ce:LYSO and Ce:GAGG matrices could be promising as high spatial resolution medical imaging, and have encouraged us to develop MPPC-based modules for use in submillimeter resolution PET scanners.

REFERENCES

[1] William W. Moses, "Trends in PET imaging", Nucl. Instr. and Meth. A 471 (2001) 209-214.

[2] Raymond R. Raylman, et al., "Initial tests of a prototype MRI-compatible PET imager", Nucl. Instr. and Meth. A 569 (2006) 306-309.

[3] Hao Peng, et al., "Proof-of-principle study of a small animal PET/field-cycled MRI combined system using conventional PMT technology", Nucl. Instr. and Meth. A 612 (2010) 412-420.

[4] Siichi Yamamoto, et al., "Design and performance from an integrated PET/MRI system for small animals", Ann Nucl Med (2010) 24:89-98

[5] Takeshi Nakamori, et al., "Development of a gamma-ray imager using a large area monolithic 4 × 4 MPPC array for a future PET scanner", JINST 7 (2012) C01083.

[6] A. Nassalski, et al., "Multi Pixel Photon Counters (MPPC) as an Alternative to APD in PET Applications", IEEE Trans. Nucl. Sci. 57 no.3 (2010) 1008-1014.

[7] Chang Lyong Kim, et al., "Multi-Pixel Photon Counters for TOF PET Detector and Its Challenges", IEEE Trans. Nucl. Sci. 56 no.5 (2009) 2580-2585.

[8] T. Kato, et al., "A novel gamma-ray detector with submillimeter resolutions using a monolithic MPPC array with pixelized Ce:LYSO and Ce:GGAG crystals", Nucl. Instr. and Meth. A, in press (2012).

[9] Seiichi Yamamoto, et al., "Development of a high-resolution Si-PM-based gamma camera system", Phys. Med. Biol., 56 (2011) 7555-7567.

[10] Seiichi Yamamoto, et al., "Development of a tweezers-type coincidence imaging detector", Ann Nucl Med (2008) 22:387-393

[11] K. Sato, et al., "Application Oriented Development of Multi-Pixel Photon Counter (MPPC)", IEEE Trans. Nucl. Sci. Conference Record, (NSS/MIC) (2010) 243-245.

[12] Ioannis G. Valais, et al., "Evaluation of the light emission efficiency of LYSO:Ce scintillator under X-ray excitation for possible applications in medical imaging", Nucl. Instr. and Meth. A 569 (2006) 201-204.

[13] Kei Kamada, et al., "2 inch diameter single crystal growth and scintillator properties of Ce:$Gd_3Al_2Ga_3O_{12}$", Journal of Crystal Growth 352 (2012) 88-90.

[14] K. Yamamoto, et al., "Development of Multi-Pixel Photon Counter (MPPC)", IEEE Trans. Nucl. Sci Conference Record, N24-292 (2007) 1511-1515.
[15] T. Kato, et al., "Development of a large-area monolithic 4×4 MPPC array for a future PET scanner employing pixelized Ce:LYSO and Pr:LuAG crystals", Nucl. Instr. and Meth. A 638 (2011) 83-91.
[16] Seiichi Yamamoto, et al., "Development of a Si-PM-based high-resolution PET system for small animals", Phys. Med. Biol. 55 (2010) 5817-5831.
[17] P. Beltrame, et al., "The AX-PET demonstrator-Design, construction and characterization", Nucl. Instr, and Meth. A 654 (2011) 546-599.
[18] Lucas Parra, et al., "List-mode likelihood: EM Algorithm and Image Quality Estimation Demonstrated on 2-D PET", IEEE Trans. Med. Imag. 17, no.2 (1998) 228-235.